

Material Instabilities in Solids

Material Instabilities in Solids

Edited by R. de BORST and E. van der GIESSEN

JOHN WILEY & SONS

Chichester · New York · Brisbane · Toronto · Singapore

Contents

14 Inelastic Deformation of F.C.C. Single Crystals By Slip and Twinning	1
14.1 Introduction	1
14.2 Constitutive Equations	2
14.2.1 Constitutive Equation For Stress	3
14.2.2 Slip and Twinning Conditions	3
14.2.3 Flow Rule	4
14.2.4 Evolution Equations For Slip and Twin Resistances	4
14.2.5 Consistency Conditions	4
14.2.6 Evolution Equations For Twin Volume Fractions	4
14.2.7 Lattice Reorientation Condition	4
14.3 Plane-Strain Deformation of F.C.C. Co-8% Fe Single Crystals	5
14.4 Concluding Remarks	10

Inelastic Deformation of F.C.C. Single Crystals By Slip and Twinning

A. Staroselsky and L. Anand

Abstract

A rate-independent constitutive model which accounts for both slip and twinning has been formulated, and a new time-integration procedure for this model has been developed. The constitutive equations and time-integration scheme have been implemented in the finite-element program ABAQUS/Explicit (1995). By using comparisons between model predictions and measured stress-strain and texture evolution data reported by Chin *et al.* (1969) for plane-strain compression of Co-8%Fe single crystals, we have deduced information about the values of the single-crystal parameters associated with slip and twin system deformation resistances for a particular crystal orientation. With the model so calibrated, we show that the predictions for the texture and stress-strain response from the model are in reasonably good agreement with experiments in plane-strain compression for a differently oriented crystal.

14.1 Introduction

The analytical modeling and computational accounting for twinning as a mechanism of plastic deformation is in its nascent stages. Some of the early considerations of twinning in crystal plasticity models are those of Chin *et al.* (1969), Chin and Mammel (1969), and Chin (1975). In these early models the shear due to twinning was treated as pseudo-slip, but the rotation due to twinning was not accounted for, and hence these models were not capable of predicting crystallographic texture evolution. Evolution of texture due to slip and twinning has been considered by Van Houtte (1978), and more recently by Tome and co-workers (e.g., Tome *et al.*, 1991; Lebensohn and Tome, 1994). However, their considerations have been for the rigid-plastic, non-hardening case, and have been limited to the Taylor (e.g., Van Houtte 1978) or the “self-consistent” (e.g., Lebensohn and Tome, 1994) averaging schemes for *polycrystalline* materials.

In this paper we report on: (i) a rate-independent elastic-plastic constitutive model which accounts for crystal plasticity by both slip and twinning, and (ii) finite element modeling to predict the operative twinning-dominated deformations and crystallographic texture evolution during plane-strain compression of face-centered-cubic (f.c.c.) *single crystals* which have been experimentally studied by Chin *et al.* (1969). We show that our model is able to reproduce reasonably the experimentally measured pole figures, and to approximate the measured stress levels during plane-strain compression of two specially oriented crystals, one in which two twin systems are operative, and another in which only one twin system is operative.

14.2 Constitutive Equations

The overall plastic deformation of a crystal is always inhomogeneous at length scales associated with slip and twinning, and should be defined as an average over a volume element that must contain enough dislocation loops and twins to result in an acceptably smooth process at the continuum level of interest here. The smallest such volume element above which the plastic response can be considered smooth, is labeled as a representative-volume element. In our model we will not account for the fine spatial structure of dislocation loops, slip bands and twin lamella in a crystal, and we shall take a *small part of a crystal* as a representative-volume element (RVE). In particular, for later use, we denote the volume fraction of twins corresponding to the i th twin system in a RVE by $f^i \geq 0$, with $\sum_i f^i \leq 1$. Also, we assume that there is no de-twinning and require that $\dot{f}^i \geq 0$.

The two major kinematic issues in modeling twinning are: (i) accounting for the shear associated with twinning; and (ii) accounting for the reorientation of the crystal lattice due to twinning. Van Houtte (1978) appears to have been the first to propose a simple tractable scheme for reorientation due to twinning. Van Houtte had limited his considerations to modeling texture development in *polycrystals*, and he chose a *whole crystal* as his RVE. In his approach, if a grain twins, then the shear due to twinning is first accumulated as a pseudo-slip, that is, the shearing rate on the twin systems is taken to be given by $\dot{\gamma}^i = \dot{f}^i \gamma_0$, where γ_0 is the amount of twinning shear, and the crystal lattice is given the twinning-related orientation only if a probabilistic

criterion, based on the relative volume fractions of the twinned and non-twinned parts of a crystal, is met. Here, we shall explore the applicability of Van Houtte's ideas to model the response of single crystals, and as mentioned previously, our RVE will be a small part of a single crystal.

A constitutive model for deformation of a single crystal by combined slip and twinning will be developed by modifying the widely used framework for crystal plasticity by slip alone. The governing variables in the constitutive model are taken as: (i) The Cauchy stress, \mathbf{T} . (ii) The deformation gradient, \mathbf{F} . (iii) Crystal slip and twin systems labeled by integers i . Each system is specified by a unit normal \mathbf{n}_0^i to the slip/twin plane, and a unit vector \mathbf{m}_0^i denoting the slip/twin direction. The slip and twin systems $(\mathbf{m}_0^i, \mathbf{n}_0^i)$ are assumed to be known in the reference configuration. The amount of shear, γ_0 , and the lattice rotation accompanying twinning, \mathbf{R}^{tw} , are also assumed to be known. (iv) A plastic deformation gradient, \mathbf{F}^p , with $\det \mathbf{F}^p = 1$. This represents the cumulative effect of dislocation motion and shear due to twinning on the active slip and twin systems in the crystal. (v) The slip and twin system deformation resistances $s^i > 0$, with units of stress. (vi) The twin fractions $f^i \geq 0$.

The elastic deformation gradient is defined by $\mathbf{F}^e \equiv \mathbf{F} \mathbf{F}^{p-1}$ with $\det \mathbf{F}^e > 0$, and it describes the elastic distortion of the lattice; it is this distortion that gives rise to the stress \mathbf{T} .

The the stress power per unit reference volume is $\dot{\omega} = \{(\det \mathbf{F}) \mathbf{T} \mathbf{F}^{-T}\} \cdot \dot{\mathbf{F}}$, which, since $\det \mathbf{F}^p = 1$, is also equal to the stress power per unit volume of the relaxed configuration determined by \mathbf{F}^p . This stress power may be additively decomposed as $\dot{\omega} = \dot{\omega}^e + \dot{\omega}^p$, where $\dot{\omega}^e = \mathbf{T}^* \cdot \dot{\mathbf{E}}^e$ is the elastic stress power per unit volume of the relaxed configuration, with

$$\mathbf{E}^e \equiv (1/2) \left\{ \mathbf{F}^{eT} \mathbf{F}^e - \mathbf{1} \right\} \quad \text{and} \quad \mathbf{T}^* \equiv (\det \mathbf{F}^e) \mathbf{F}^{e-1} \mathbf{T} \mathbf{F}^{e-T} \quad (14.1)$$

the Green elastic strain measure and the symmetric second Piola-Kirchoff stress tensor relative to the relaxed configuration, respectively; and

$$\dot{\omega}^p = (\mathbf{C}^e \mathbf{T}^*) \cdot \left(\dot{\mathbf{F}}^p \mathbf{F}^{p-1} \right), \quad \mathbf{C}^e \equiv \mathbf{F}^{eT} \mathbf{F}^e, \quad (14.2)$$

is the plastic stress power per unit volume of the relaxed configuration.

14.2.1 Constitutive Equation For Stress

Elastic stretches in metallic single crystals are generally small. Accordingly, the constitutive equation for the stress in a metallic single crystal is taken as the linear relation

$$\mathbf{T}^* = \mathcal{C} [\mathbf{E}^e], \quad (14.3)$$

where \mathcal{C} is a fourth-order anisotropic elasticity tensor, where \mathbf{E}^e and \mathbf{T}^* are the strain and stress measures defined in equation (14.1).

14.2.2 Slip and Twinning Conditions

Let

$$\mathbf{S}_0^i = \mathbf{m}_0^i \otimes \mathbf{n}_0^i \quad (14.4)$$

denote the Schmid tensors, and consistent with equation (14.2), and let

$$\tau^i = (\mathbf{C}^e \mathbf{T}^*) \cdot \mathbf{S}_0^i \quad (14.5)$$

denote the resolved shear stress on the i th slip/twin system. Then, the conditions for slip and twinning are taken as

$$\phi^i = |\tau^i| - s^i = 0. \quad (14.6)$$

14.2.3 Flow Rule

The evolution of the plastic deformation gradient is

$$\dot{\mathbf{F}}^p = \mathbf{L}^p \mathbf{F}^p, \quad (14.7)$$

with \mathbf{L}^p given by the sum of the shearing rates on all the slip and twin systems

$$\mathbf{L}^p = \sum_i \dot{\gamma}^i \text{sign}(\tau^i) \mathbf{S}_0^i. \quad (14.8)$$

The shearing rates are restricted as follows:

$$\dot{\gamma}^i \geq 0, \quad \text{and} \quad \dot{\gamma}^i \phi^i = 0. \quad (14.9)$$

14.2.4 Evolution Equations For Slip and Twin Resistances

These may be generically taken as

$$\dot{s}^i = \sum_j h^{ij} \dot{\gamma}^j, \quad (14.10)$$

where h^{ij} are the hardening moduli. However, in this paper we shall only consider the non-hardening case with $h^{ij} = 0$ (see Sec. 1.3 below).

14.2.5 Consistency Conditions

During plastic flow the following consistency conditions must be satisfied:

$$\dot{\gamma}^i \dot{\phi}^i = 0 \quad \text{if} \quad \phi^i = 0. \quad (14.11)$$

The consistency conditions serve to determine the shearing rates $\dot{\gamma}^i \geq 0$ on the slip and twin systems.

14.2.6 Evolution Equations For Twin Volume Fractions

For the twin systems,

$$\dot{f}^i = \dot{\gamma}^i / \gamma_0 \geq 0, \quad (14.12)$$

where γ_0 is the twinning shear.

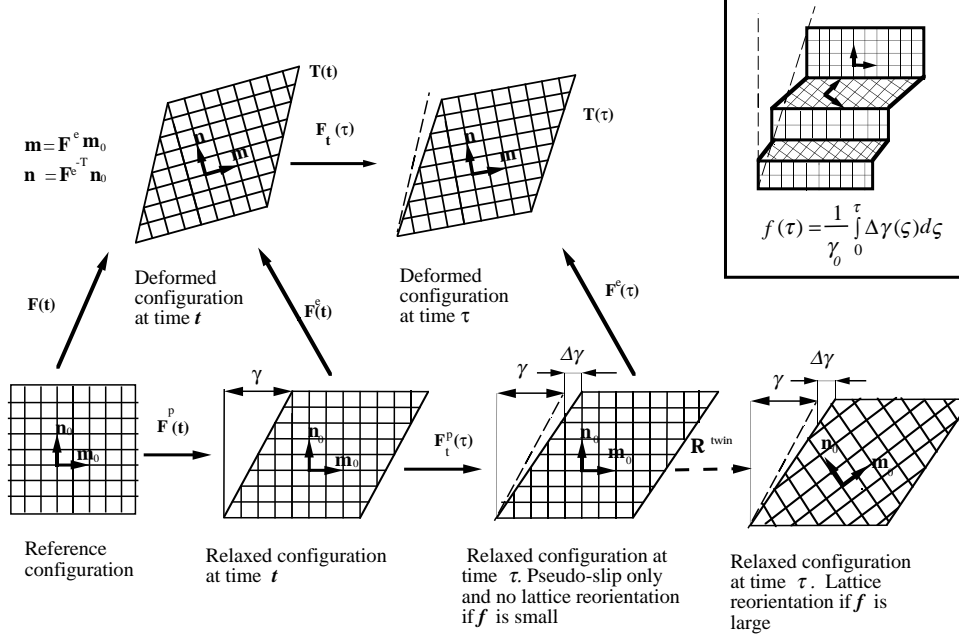


Figure 14.1 Schematic of the incremental kinematics of slip and twinning.

14.2.7 Lattice Reorientation Condition

Let f denote the volume fraction of the twin system with the maximum value of f^i at a given time t , and let $\xi = 0.3$ denote a representative maximum value of f in a RVE. The lattice reorientation condition suggested by Van Houtte (1978), and adopted here, is that if $f > \xi$, then the orientation of the RVE be replaced by the twin related orientation¹. That is, if $\{\mathbf{e}_i^c | i = 1, 2, 3\}$ denotes a local orthonormal basis associated with the crystal lattice in the old relaxed configuration, then once this criterion is met the crystal basis in the new relaxed configuration of the crystal be taken as $\mathbf{e}_i^{c*} = \mathbf{R}^{\text{tw}} \mathbf{e}_i^c$. To fix ideas, a schematic of the incremental kinematics of slip and twinning outlined above is shown in Fig. 14.1.

Further, if the lattice reorientation condition is met, then the f^i are reinitialized to zero, and subsequent twinning in the RVE is suppressed by setting the twin system deformation resistances to a large value. However, subsequent slip in this RVE is allowed, and the values of all slip system resistances are set equal to the value of the resistance for the slip system(s) parallel to the twin system with the maximum f^i prior to the reorientation.

A time-integration procedure for the constitutive equations is outlined in the Appendix. The constitutive equations and the time-integration procedure have been implemented in the finite-element program ABAQUS/Explicit (1995) by writing a “user material” subroutine. The single-crystal calculations shown in the following section were carried out by modeling a part of a single crystal as a single finite element.

¹ Van Houtte actually suggested use of a probabilistic criterion with $\xi \in [0.3, 1]$ denoting a random number. Also, the fraction 0.3 is only an approximate number.

14.3 Plane-Strain Deformation of F.C.C. Co-8% Fe Single Crystals

The elastic constants for Co-8% Fe single crystals are taken to be the same as that for Co (Simmons and Wang, 1971):

$$C_{11} = 260 \text{ GPa}, C_{12} = 150 \text{ GPa}, C_{44} = 78 \text{ GPa}.$$

Slip in f.c.c. crystals occurs on twelve $\{111\} \langle 110 \rangle$ slip systems listed in Table 14.1. Note that on a given slip system, slip can occur in either the positive or negative $\langle 110 \rangle$ slip direction in a $\{111\}$ plane.

Table 14.1 The Twelve $\{111\} \langle 110 \rangle$ Slip Systems

$[0\bar{1}\bar{1}]$	(111) $[\bar{1}01]$	$[1\bar{1}0]$	$[0\bar{1}\bar{1}]$	$(\bar{1}\bar{1}\bar{1})$ $[\bar{1}01]$	$[\bar{1}10]$	$[01\bar{1}]$	$(\bar{1}11)$ $[\bar{1}01]$	$[\bar{1}\bar{1}0]$	$[0\bar{1}\bar{1}]$	$(1\bar{1}\bar{1})$ $[\bar{1}01]$	$[110]$
---------------------	--------------------------	---------------	---------------------	--------------------------------------------	---------------	---------------	--------------------------------	---------------------	---------------------	--------------------------------------	---------

Twinning in f.c.c. crystals occurs on twelve $\{111\} \langle 11\bar{2} \rangle$ twin systems listed in Table 14.2 (e.g., Kelly and Groves, 1970). Note that unlike the slip systems listed in Table 14.1 for which slip can occur in either the positive or negative $\langle 110 \rangle$ slip direction in a $\{111\}$ plane, twinning, because the underlying atomic arrangement is polar in nature, can occur in only one $\langle 11\bar{2} \rangle$ type direction on a $\{111\}$ plane, and the twin systems listed in Table 14.2 correspond to the easy direction of twinning. We do not consider the possibility of “de-twinning” in this paper.

Table 14.2 The Twelve $\{111\} \langle 11\bar{2} \rangle$ Twin Systems

$[211]$	(111) $[\bar{1}21]$	$[11\bar{2}]$	$[2\bar{1}\bar{1}]$	$(\bar{1}\bar{1}\bar{1})$ $[\bar{1}21]$	$[\bar{1}\bar{1}\bar{2}]$	$[211]$	(111) $[\bar{1}21]$	$[\bar{1}1\bar{2}]$	$[2\bar{1}\bar{1}]$	$(1\bar{1}\bar{1})$ $[\bar{1}21]$	$[11\bar{2}]$
---------	--------------------------	---------------	---------------------	--------------------------------------------	---------------------------	---------	--------------------------	---------------------	---------------------	--------------------------------------	---------------

The twinning shear corresponding to a twin system may be written as

$$\mathbf{1} + \gamma_0 \mathbf{m}_0 \otimes \mathbf{n}_0, \quad \mathbf{m}_0 \cdot \mathbf{n}_0 = 0, \quad \gamma_0 = 1/\sqrt{2}, \quad (14.13)$$

where \mathbf{m}_0 is a unit vector in a $\langle 11\bar{2} \rangle$ direction, and \mathbf{n}_0 the unit normal to the associated $\{111\}$ plane. The corresponding twinning rotation is given by

$$\mathbf{R}^{tw} = 2 \mathbf{n}_0 \otimes \mathbf{n}_0 - \mathbf{1}. \quad (14.14)$$

Henceforth, to distinguish the slip and twin resistances, we adopt the notation s^i and s^α to denote the slip and twin resistances, respectively. The initial values of these resistances are denoted by s_0^i and s_0^α .

Representation of the slip-twin hardening and hardening interactions is one of the major uncertainties, and much work needs to be done to improve our understanding of these hardening interactions and their mathematical representation. In this preliminary study, we shall concentrate more on lattice reorientation due to slip and twinning during plane-strain compression of the crystals, and we will pay only marginal attention to the details of the stress-strain response. Accordingly, during the “pseudo-slip” phase, the slip and twin system deformation resistances will be taken as constant. Leffers and co-workers (e.g., 1991, 1993) have reported that during plane-strain compression of brass, twins form thin lamellae which cluster to form bundles in grains, and that subsequent slip is restricted to planes which are parallel to these twin bundles. We have modeled this important kinematic restriction on the activity of the slip systems as follows. When the fraction $f = \max \{f^\alpha\}$, the maximum value of f^α taken over all twin systems, reaches a value $\lambda \approx 0.05$, slipping and twinning in systems whose slip/twin planes are not parallel to the plane of the twin system with maximum f^α are restricted by choosing appropriate values of slip and twin resistances. Let \mathcal{T}_λ denote the single-element set denoting the twin system for which f^α reaches the value λ , with corresponding resistance $s_{tw,\lambda}$. Also, let \mathcal{S}_λ denote the set of slip systems which are parallel to this twin system. Then $s_{tw,\lambda}$ is still taken to be equal to its initial value $s_{tw,\lambda} = s_{tw,0}$, however for the other twinning systems, setting

$$s^\alpha = 5 \times s_{tw,0} \quad \text{for } \alpha \notin \mathcal{T}_\lambda, \quad (14.15)$$

renders them inoperative. Similarly, for the slip systems we require

$$\begin{aligned} s^i(\tau) &= s_0^i & \text{for } i \in \mathcal{S}_\lambda, \\ s^i &= 5 \times s_0^i & \text{for } i \notin \mathcal{S}_\lambda. \end{aligned} \quad (14.16)$$

We shall simulate plane-strain compression of two specially oriented single crystals Co-8%Fe tested by Chin *et al.* (1969). A schematic of plane-strain compression in a channel-die fixture is shown in Fig. 14.2. In the metallurgical literature, the geometry of such experiments is typically described by a pair of Miller indices $(hkl)[uvw]$, where (hkl) denotes the Miller indices of the crystallographic plane parallel to the compression plane with outward unit normal \mathbf{e}_2 , as shown in Fig. 14.2, and $[uvw]$ denotes the Miller indices of the crystallographic direction parallel to the free direction, \mathbf{e}_1 in Fig. 14.2. The particular orientations of the crystals experimentally studied by Chin *et al.* (1969) that we have chosen to simulate in this paper are $(110)[\bar{3}34]$ and $(335)[\bar{5}\bar{5}6]$. These initial crystal orientations may alternatively be described in terms of the Euler angle notation $\{\theta, \phi, \omega\}$ of Kalidindi *et al.* (1992); these Euler angles are listed in Table 14.3.

Table 14.3 Single crystal orientations specified by Euler angles

Orientation	θ	ϕ	ω
$(110)[\bar{3}34]$	43.31	45	270
$(335)[\bar{5}\bar{5}6]$	90	225	40.32

For the numerical simulation of plane-strain compression, 900 two-dimensional ABAQUS-CPE4R elements (continuum, plane-strain, 4-noded, reduced integration)

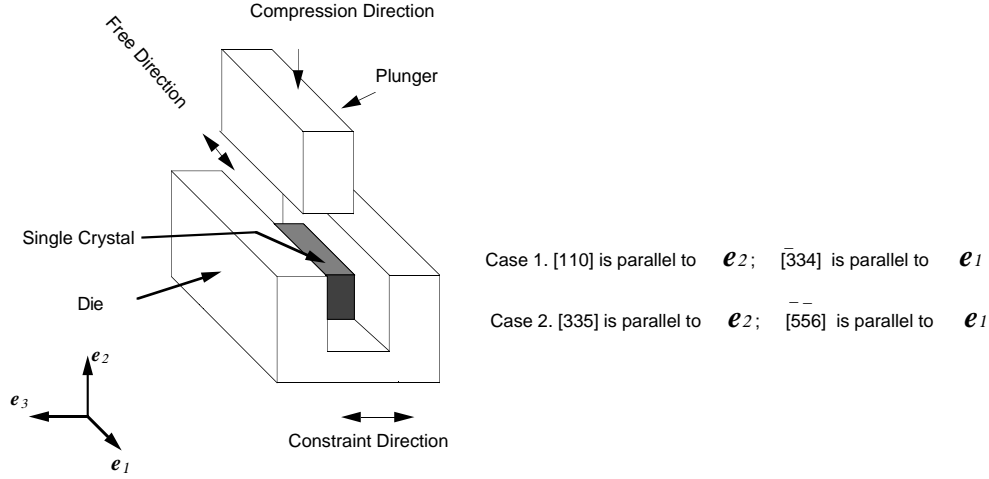


Figure 14.2 Schematic of plane-strain compression experiments.

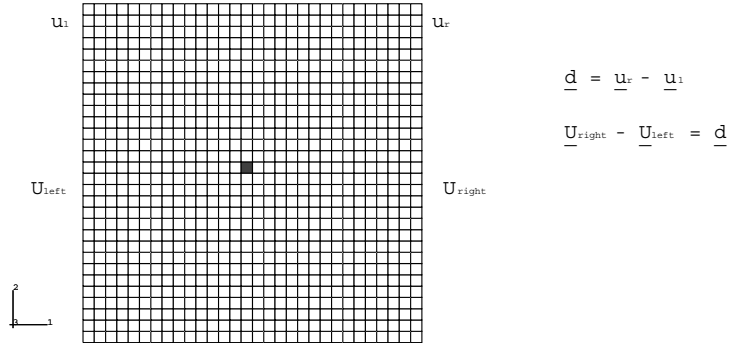


Figure 14.3 Initial finite element mesh. Each finite element represents a RVE.

were assigned to the single crystal. Fig. 14.3 shows the initial mesh geometry. It is important to note that our 2-D finite element simulations incorporate the full 3-D slip and twin system structure. With respect to Fig. 14.3, plane-strain compression was modeled by constraining the top and bottom boundaries of the mesh to remain straight, with the bottom boundary subjected to zero displacement in the 2-direction, and top boundary subjected to a negative displacement in the 2-direction for a total compressive strain of 20%. For the vertical boundaries we imposed periodic boundary conditions, defined as follows. Let \mathbf{u}_l and \mathbf{u}_r respectively denote the displacements for a node on the left boundary and another on the right boundary which is at the same horizontal level in the initial mesh, and let $\mathbf{d} = \mathbf{u}_r - \mathbf{u}_l$ denote the relative displacement for this pair of corresponding nodes on the left and right boundaries. Then, partially periodic boundary conditions are specified by requiring that $\mathbf{U}_{right} - \mathbf{U}_{left} = \mathbf{d}$, where \mathbf{U}_{left} and \mathbf{U}_{right} are the vectors of displacements of all the nodes for the left and right boundaries, respectively.

In the numerical simulations reported below, we have used the following values for

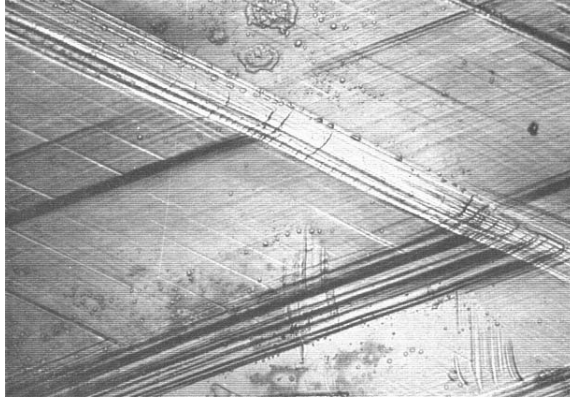


Figure 14.4 Micrograph of the $(110)[\bar{3}34]$ oriented crystal showing twin bands (from Chin *et al.*, 1969).

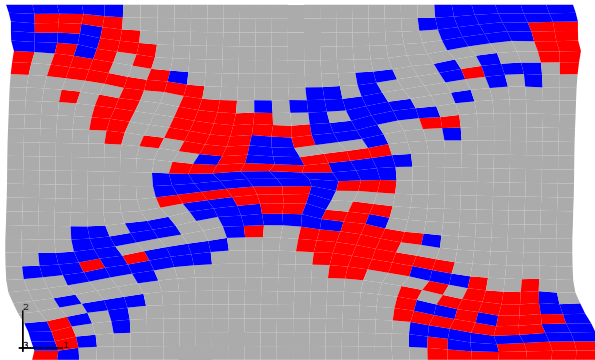


Figure 14.5 The deformed FEM mesh with calculated twin bands.

the slip and twin resistances:

$$s_0^i = 70 \text{ MPa}; \quad s_0^a = 40 \text{ MPa}.$$

We first simulated plane-strain compression of a $(110)[\bar{3}34]$ oriented crystal. A micrograph of the deformed specimen taken from Chin *et al.* (1969) is shown in Fig. 14.4. This picture shows that a mixture of slip and twinning has occurred on the (111) and $(11\bar{1})$ planes. Our corresponding finite element simulation is shown in Fig. 14.5. Our calculations also predict that slip occurs on the $(111)[\bar{1}01]$ and $(11\bar{1})[0\bar{1}\bar{1}]$ systems, and twinning occurs on the $(111)[\bar{1}21]$ and $(\bar{1}\bar{1}1)[\bar{1}21]$ systems. The elements twinned by the $(111)[\bar{1}21]$ system are shaded black, and those twinned by the $(\bar{1}\bar{1}1)[\bar{1}21]$ system are shaded dark grey. The calculated twin bands intersect at an angle close to that observed in the experiments (Fig. 14.4).

Texture evolution is one of the most important characteristics of slip/twin systems activity. Fig. 14.6(a) presents the $\{111\}$ pole figure² of the crystal in its initial orientation. The pole figure predicted by the finite element calculations is shown in Fig. 14.6(b), together with the experimentally measured (Chin *et al.*, 1969) pole figure in Fig. 14.6(c). The agreement between numerically predicted and experimentally

² All pole figures shown are in stereographic projection.

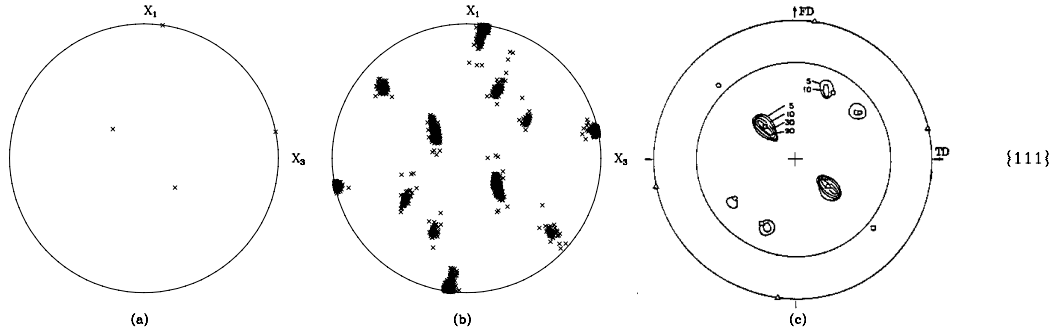


Figure 14.6 $\{111\}$ pole figures for $(110)[\bar{3}34]$ oriented crystal. Initial (a), FEM calculated after plane-strain compression to 20% (b), and experimentally measured (Chin *et al.*, 1969) (c).

measured texture is very good.

The stress-strain data of Chin *et al.* (1969) is shown in Fig.14.7. Note that they do

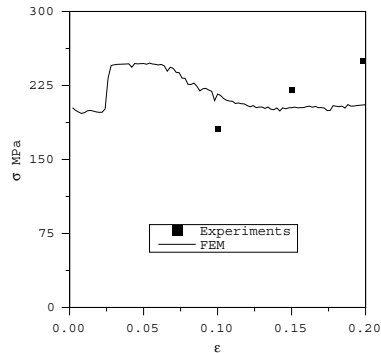


Figure 14.7 Stress-strain data for plane-strain compression of $(110)[\bar{3}34]$ oriented crystal.

not report data for strains less than $\approx 10\%$. It was this stress-strain data which was chosen to estimate the slip and twin resistances used in our numerical simulations. The computed stress-strain curve is also shown in Fig. 14.7. Overall the computed stress levels are in the range of that observed in the experiments. The first part of the curve up to strains of less than $\approx 2.5\%$ corresponds to the general plastic deformation by combined slip and twinning with twinning treated as pseudo-slip. The sudden jump in the stress at a strain of approximately 2.5% corresponds to the attainment of the first threshold when slip in certain elements is constrained to be operative on slip systems which are parallel to the dominant twin systems. The subsequent drops in stresses in the calculated stress-strain curve correlate with the reorientation of the crystallographic lattices of elements due to twinning. Note that if we were to increase substantially the number of elements used in the finite element simulation, then the computed curve would be smoother.

Next, we simulated plane-strain compression of a $(335)[\bar{5}\bar{5}6]$ oriented crystal. A micrograph of the deformed specimen taken from Chin *et al.* (1969) is shown in Fig.

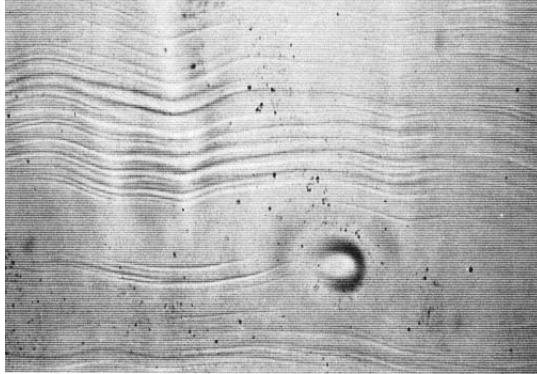


Figure 14.8 Micrograph of the $(335)[\bar{5}\bar{5}6]$ oriented crystal showing twin bands (from Chin *et al.*, 1969).

14.8. Chin *et al.* report that during the early stages of deformation, slip on $(111)[\bar{1}\bar{1}0]$ and $(\bar{1}\bar{1}1)[\bar{1}\bar{1}0]$ systems predominated. With increasing deformation, twinning on $(111)[11\bar{2}]$ became predominant. Our calculations in Fig.14.9 show the same twin system, $(111)[11\bar{2}]$, to be dominant at a strain of 20%. The twinned elements in the

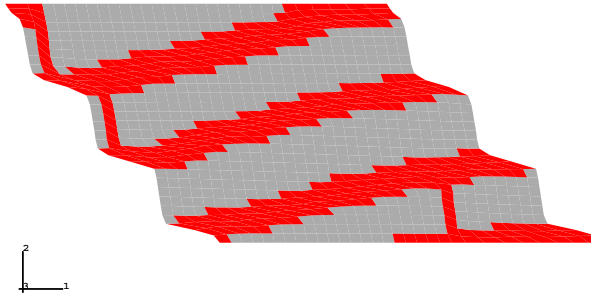


Figure 14.9 The deformed FEM mesh with calculated twin bands.

deformed finite element mesh are shaded black. Because of the activation of only one twin system, the macroscopic shear deformations became significant and the mesh was visibly sheared.

The $\{111\}$ pole figure for the initial orientation is shown in Fig.14.10(a). The calculated and experimentally measured (Chin *et al.*, 1969) textures after plane-strain compression to 20% are shown in Figs. 14.10(b) and 14.10(c), respectively. As for the previous calculation, the calculated texture captures the main features of the experimental texture. The calculated stress-strain curve together with the experimental data by Chin *et al.* (1969) is shown in Fig.14.11. The calculated stress levels are in the right range.

14.4 Concluding Remarks

Our calculations clearly demonstrate the ability of our constitutive model and computational procedure to capture the major features of plastic deformation of a

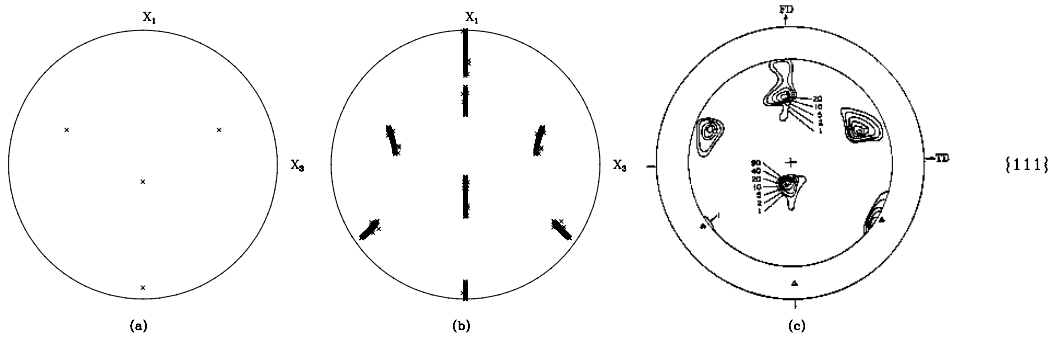


Figure 14.10 $\{111\}$ pole figures for $(335)[\bar{5}\bar{5}6]$ oriented crystal. Initial (a), FEM calculated after plane-strain compression to 20% (b), and experimentally measured (Chin *et al.*, 1969) (c).

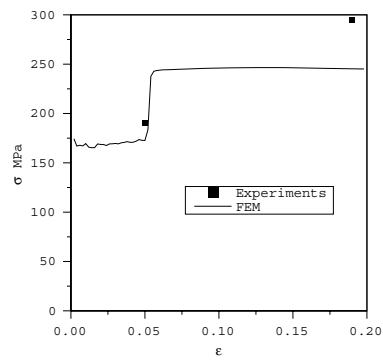


Figure 14.11 Stress-strain data for plane-strain compression of $(335)[\bar{5}\bar{5}6]$ oriented crystal.

single crystal due to slip and twinning. However, as formulated, the constitutive model has a number of limitations: (i) The model at this stage is essentially non-hardening. (ii) The important role of twin-boundary energy is neglected in the model. (iii) There is no length scale in the model. Much work needs to be done to improve our understanding of the slip and twin hardening and hardening interactions, and their mathematical representation.

The limitations in the finite element calculations are mostly related to our use of a small number of elements. Because of the coarse mesh, the twin bands propagate at an angle that is determined not only by the underlying slip and twin systems, but also by the finite element mesh itself. A more refined mesh should mitigate this problem. However, the problem of the width of the twin bands is not solved by refining the mesh. For this, a suitable length scale associated with non-local effects of twinning needs to be introduced into the constitutive model.

Acknowledgements

The support for this work was provided by the U.S. Army Research Office under Grant DAAH04-94-G-0060, and the National Science Foundation under Grant CMS-9610130. The ABAQUS finite element software was made available under an academic license from HKS, Inc., Pawtucket, R.I.

References

- ABAQUS (1995) *Reference Manuals*. Hibbitt, Karlsson, & Sorensen Inc., Pawtucket, R.I.
- Anand, L., and Kothari, M. (1996) A Computational Procedure For Rate-Independent Plasticity. *Journal of The Mechanics and Physics of Solids*, **44**, 525-558.
- Chin, G. Y., Hosford, W. F., and Mendorf, D. R. (1969), Accommodation of Constrained Deformation in f.c.c. Metals by Slip and Twinning. *Proceedings of The Royal Society A*, **309**, 433-456.
- Chin, G. Y., and Mammel, W. L. (1969) Generalization and Equivalence of the Minimum Work (Taylor) and Maximum Work (Bishop-Hill) Principles of Crystal Plasticity. *Transactions of AIME*, **245**, 1211 – 1214.
- Chin, G. Y. (1975) Development of Deformation Textures, in *Constitutive Equations in Plasticity*, Argon, A. S., ed., 431 – 447.
- Kelly, A., and Groves, G. W., (1970) *Crystallography and Crystal Defects*, Longman, London, 290 – 312.
- Lebensohn, R. A., and Tome, C. N. (1994) A Self-Consistent Viscoplastic Model: Prediction of Rolling Textures of Anisotropic Polycrystals. *Materials Science and Engineering*, **A175**, 71 – 82.
- Leffers, T. (1991) Microstructures, Textures, and Deformation Patterns at Large Strain. In *MECAMAT'91*, Balkema, Rotterdam, 73-86.
- Leffers, T., and Bilde-Sorensen, J. B. (1990) Intra- and Intergranular Heterogeneities in Plastic Deformation of Brass During Rolling. *Acta Metallurgica et Materialia*, **38**, 1917-1926.

- Leffers, T. and Jensen, D. J. (1993) in *Textures and Microstructures*, **14-18**, 933-952.
- Simmons, G., and Wang, H. (1971) *Single Crystal Elastic Properties and Calculated Aggregate Properties: A HANDBOOK*. The MIT Press, Cambridge, USA.
- Tome, C. N., Lebensohn, R. A., and Kocks, U. F. (1991) A Model for Texture Development Dominated by Deformation Twinning: Application to Zirconium Alloys. *Acta Metallurgica et Materialia*, **39**, 2667 – 2680.
- Van Houtte, P. (1978) Simulation of the Rolling and Shear Texture of Brass by the Taylor Theory adapted for Mechanical Twinning. *Acta Metallurgica*, **26**, 591 – 604.

APPENDIX

Here we summarize a time-integration procedure for our rate-independent single crystal constitutive model. With t denoting the current time, Δt is an infinitesimal time increment, and $\tau = t + \Delta t$. The algorithm is as follows:

Given: (1) $\{\mathbf{F}(t), \mathbf{F}(\tau)\}$; (2) $\{\mathbf{T}(t), \mathbf{F}^p(t)\}$; (3) a rotation tensor $\bar{\mathbf{Q}}(t)$, which brings an orthonormal basis $\{\mathbf{e}_i^{(c)}(t)\}$ associated with the crystal to be in correspondence with a fixed orthonormal basis $\{\mathbf{e}_i^{(g)}\}$ in space; (4) $\{\mathbf{m}_o^i(t), \mathbf{n}_o^i(t), s^i(t)\}$; and (5) the accumulated shears due to twinning $\Gamma^i(t)$, where the index i ranges over the previously active twin systems since the last reorientation of the lattice.

Calculate: (a) $\{\mathbf{T}(\tau), \mathbf{F}^p(\tau)\}$; (b) the accumulated shears due to twinning $\Gamma^i(\tau)$, where the index i ranges over the previously active twin systems since the last reorientation of the lattice; (c) the rotation tensor $\bar{\mathbf{Q}}(\tau)$, which brings the orthonormal crystal basis $\{\mathbf{e}_i^{(c)}(\tau)\}$ to be in correspondence with a fixed orthonormal basis $\{\mathbf{e}_i^{(g)}\}$ in space; (d) $\{\mathbf{m}_o^i(\tau), \mathbf{n}_o^i(\tau), s^i(\tau)\}$; and (e) the orientation of the slip and systems in the deformed configuration at time τ from

$$\mathbf{m}_\tau^i = \mathbf{F}^e(\tau)\mathbf{m}_o^i(\tau), \quad \mathbf{n}_\tau^i = \mathbf{F}^e(\tau)^{-T}\mathbf{n}_o^i(\tau).$$

The steps used in the calculation procedure are:

Step 1. Calculate a trial elastic strain $\mathbf{E}^e(\tau)^{tr}$:

$$\begin{aligned} \mathbf{F}^e(\tau)^{tr} &= \mathbf{F}(\tau)\mathbf{F}^p(t)^{-1}, \\ \mathbf{C}^e(\tau)^{tr} &= (\mathbf{F}^e(\tau)^{tr})^T\mathbf{F}^e(\tau)^{tr}, \\ \mathbf{E}^e(\tau)^{tr} &= (1/2)\{\mathbf{C}^e(\tau)^{tr} - \mathbf{1}\}. \end{aligned}$$

Step 2. Calculate a trial stress $\mathbf{T}^*(\tau)^{tr}$:

$$\mathbf{T}^*(\tau)^{tr} = \mathcal{C}[\mathbf{E}^e(\tau)^{tr}].$$

Step 3. Calculate a trial resolved shear stress $\tau^i(\tau)^{tr}$ on each slip and twin system. Recall that the resolved shear stress was defined as $\tau(\tau) = \{\mathbf{C}^e(\tau)\mathbf{T}^*(\tau)\} \cdot \mathbf{S}_0(t)$, where $\mathbf{S}_0(t) = \mathbf{m}_0(t) \otimes \mathbf{n}_0(t)$. For infinitesimal elastic stretches the resolved shear stress $\tau(\tau)$ may be approximated by $\tau(\tau) \doteq \mathbf{T}^*(\tau) \cdot \mathbf{S}_0(t)$. Accordingly, the trial resolved shear stress is calculated as

$$\tau^i(\tau)^{tr} = \mathbf{T}^*(\tau)^{tr} \cdot \mathbf{S}_0^i(t).$$

Step 4. Determine the set \mathcal{PA} of potentially active slip and twin systems which satisfy

$$|\tau^i(\tau)^{tr}| - s^i(t) > 0.$$

Step 5. We shall use the following incremental versions of the flow rule and the evolution equations for the slip and twin systems resistances:

$$\mathbf{F}^p(\tau) = \left\{ \mathbf{1} + \sum_{i \in \mathcal{PA}} \Delta\gamma^i \text{sign}(\tau^i(\tau)^{\text{tr}}) \mathbf{S}_0^i(t) \right\} \mathbf{F}^p(t)$$

$$s^i(\tau) = s^i(t) + \sum_{j \in \mathcal{PA}} h^{ij}(t) \Delta\gamma^j, \quad i = 1, \dots, N, \quad (14.17)$$

where N is the total number of slip and twin systems.

During plastic flow the active systems must satisfy the consistency condition

$$|\tau^i(\tau)| = s^i(\tau). \quad (14.18)$$

A calculation for $|\tau^i(\tau)|$, retaining terms of first order in $\Delta\gamma^j$, gives

$$|\tau^i(\tau)| = \left| \tau^i(\tau)^{\text{tr}} \right| - \sum_{i \in \mathcal{PA}} \left\{ \text{sign}(\tau^i(\tau)^{\text{tr}}) \text{sign}(\tau^j(\tau)^{\text{tr}}) \mathbf{S}_0^i(t) \cdot \mathcal{C} \left[\text{sym}(\mathbf{C}^e(\tau)^{\text{tr}} \mathbf{S}_0^j(t)) \right] \right\} \Delta\gamma^j. \quad (14.19)$$

Use of (14.17) and (14.19) in the consistency condition (14.18) gives

$$\sum_{j \in \mathcal{PA}} A^{ij} x^j = b^i, \quad i \in \mathcal{PA}, \quad (14.20)$$

with

$$A^{ij} = h^{ij} + \text{sign}(\tau^i(\tau)^{\text{tr}}) \text{sign}(\tau^j(\tau)^{\text{tr}}) \mathbf{S}_0^i(t) \cdot \mathcal{C} \left[\text{sym}(\mathbf{C}^e(\tau)^{\text{tr}} \mathbf{S}_0^j(t)) \right], \quad (14.21)$$

$$b^i = \left| \tau^i(\tau)^{\text{tr}} \right| - s^i(t) > 0, \quad (14.22)$$

$$x^j \equiv \Delta\gamma^j \geq 0. \quad (14.23)$$

Equation (14.20) is a system of linear equations for $x^j \equiv \Delta\gamma^j \geq 0$, with the matrix A possibly singular.

For the case of slip alone, Anand and Kothari (1996) have recently proposed an iterative solution procedure based on the Singular Value Decomposition (SVD) of A to determine the active slip systems and the corresponding shear increments. In their procedure the shear increments are calculated as

$$x^+ = A^+ b,$$

where A^+ is the pseudo-inverse of the matrix of the matrix A , defined over all the potentially active slip and twin systems. If A is singular, then from the set of non-unique solutions to $Ax = b$, the chosen solution is the one which has the minimum length $\|x\|_2$. If for any system the solution $x^j = \Delta\gamma^j \leq 0$, then this system is inactive, and it is removed from the set of potentially active systems. The reduced system $Ax = b$ is solved again using the pseudo-inverse of the new A . This iterative procedure is continued until all $x^j = \Delta\gamma^j > 0$.

Step 6. Update the plastic deformation gradient $\mathbf{F}^p(\tau)$:

$$\mathbf{F}^p(\tau) = \left\{ \mathbf{1} + \sum_{i \in \mathcal{A}} \text{sign}(\tau^i(\tau)^{\text{tr}}) \Delta\gamma^i \mathbf{S}_o^i(t) \right\} \mathbf{F}^p(t).$$

Step 7. Check if $\det \mathbf{F}^p(\tau) = 1$. If not, normalize $\mathbf{F}^p(\tau)$ as :

$$\mathbf{F}^p(\tau) = [\det \mathbf{F}^p(\tau)]^{-1/3} \mathbf{F}^p(\tau).$$

Step 8. Compute the elastic deformation gradient $\mathbf{F}^e(\tau)$ and the stress $\mathbf{T}^*(\tau)$:

$$\begin{aligned} \mathbf{F}^e(\tau) &= \mathbf{F}(\tau) \mathbf{F}^p(\tau)^{-1} \\ \mathbf{T}^*(\tau) &= \mathcal{C}[\mathbf{E}^e(\tau)]. \end{aligned}$$

Step 9. Update the variables $\{\mathbf{T}(\tau), s^i(\tau)\}$:

$$\begin{aligned} \mathbf{T}(\tau) &= \mathbf{F}^e(\tau) \{[\det \mathbf{F}^e(\tau)]^{-1} \mathbf{T}^*(\tau)\} \mathbf{F}^{eT}(\tau) \\ s^i(\tau) &= s^i(t) + \sum_{j \in \mathcal{A}} h^{ij} \Delta\gamma^j, \quad i = 1, \dots, N \end{aligned}$$

Step 10. Update the accumulated shears due to twinning and the twin fractions:

$$\begin{aligned} \Gamma^i(\tau) &= \Gamma^i(t) + \Delta\gamma^i, \\ f^i(\tau) &= \Gamma^i(\tau) / \gamma_0, \end{aligned}$$

where the index i ranges over all the active twin systems.

Step 11. Rotate the lattice if a sufficiently large fraction of the RVE has twinned. Let $f(\tau) = \max\{f^i(\tau)\}$ denote the maximum value of the twin fraction, and let $\xi = 0.3$. If $f(\tau) > \xi$, then set $\bar{\mathbf{Q}}(\tau) = \bar{\mathbf{Q}}(t) (\mathbf{R}^{tw}(t))^T$.

Step 12. Calculate the “texture” $(\mathbf{m}_\tau^i, \mathbf{n}_\tau^i)$:

$$\begin{aligned} \mathbf{m}_\tau^i &= \mathbf{F}^e(\tau) \mathbf{m}_0^i, \\ \mathbf{n}_\tau^i &= \mathbf{F}^{e-T}(\tau) \mathbf{n}_0^i. \end{aligned}$$

The single-crystal constitutive equations and the time-integration procedures described in this section have been implemented in the finite-element program ABAQUS/Explicit (1995) by writing a “user material” subroutine.